A Measurement of $\sin^2\theta_{\mathrm{W}}$ in νN Scattering from NuTeV

G. P. Zeller[5], T. Adams[4], A. Alton[4], S. Avvakumov[7], L. de Barbaro[5], P. de Barbaro[7], R. H. Bernstein[3], A. Bodek[7], T. Bolton[4], J. Brau[6], D. Buchholz[5], H. Budd[7], L. Bugel[3], J. Conrad[2], R. B. Drucker[6], J. Formaggio[2],R. Frey[6], J. Goldman[4], M. Goncharov[4], D. A. Harris[7], R. A. Johnson[1], S. Koutsoliotas[2], J. H. Kim[2], M. J. Lamm[3], W. Marsh[3], D. Mason[6], C. McNulty[2], K. S. McFarland[7,3], D. Naples[4], P. Nienaber[3], A. Romosan[2], W. K. Sakumoto[7], H. Schellman[5], M. H. Shaevitz[2], P. Spentzouris[2], E. G. Stern[2], B. Tamminga[2], M. Vakili[1], A. Vaitaitis[2], V. Wu[1], U. K. Yang[7] and J. Yu[3]

[1] *University of Cincinnati, Cincinnati, OH 45221*
[2] *Columbia University, New York, NY 10027*
[3] *Fermi National Accelerator Laboratory, Batavia, IL 60510*
[4] *Kansas State University, Manhattan, KS 66506*
[5] *Northwestern University, Evanston, IL 60208*
[6] *University of Oregon, Eugene, OR 97403*
[7] *University of Rochester, Rochester, NY 14627*

The NuTeV experiment at Fermilab presents a determination of the electroweak mixing angle. High purity, large statistics samples of $\nu_\mu N$ and $\overline{\nu}_\mu N$ events allow the use of the Paschos-Wolfenstein relation. This considerably reduces systematic errors associated with charm production and other sources. With Standard Model assumptions, this measurement of $\sin^2\theta_W$ indirectly determines the W boson mass to a precision comparable to direct measurements from high energy e^+e^- and $p\bar{p}$ colliders. NuTeV measures $\sin^2\theta_{\mathrm{W}}^{(\mathrm{on-shell})} = 0.2253 \pm 0.0019(\mathrm{stat.}) \pm 0.0010(\mathrm{syst.})$, which implies $M_W = 80.26 \pm 0.11$ GeV.

I. INTRODUCTION

Neutrino scattering experiments have contributed to our understanding of electroweak physics for more than three decades. Early determinations of $\sin^2\theta_W$ served as the critical ingredient to the Standard Model's successful prediction of the W and Z boson masses. More precise investigations in the late 1980's set the first useful limits on the top quark mass. Just as early measurements contributed to the accurate predictions of the W, Z, and top quark masses before their direct observation, recent results from neutrino-scattering experiments combined with e^+e^- and $p\bar{p}$ collider data likewise constrain the Higgs boson mass.

The measurement presented here represents the most precise determination of the electroweak mixing angle from neutrino-nucleon scattering to date. The result is a factor of two more precise than the previous most accurate νN measurement [1].

II. METHODOLOGY

In deep inelastic neutrino-nucleon scattering, the weak mixing angle can be extracted from the ratio of neutral current (NC) to charged current (CC) total cross sections. Previous measurements relied on the Llewellyn-Smith formula, which relates these ratios to $\sin^2\theta_W$ for neutrino scattering on isoscalar targets [2]:

$$R^\nu \equiv \frac{\sigma(\nu_\mu N \to \nu_\mu X)}{\sigma(\nu_\mu N \to \mu^- X)} = \frac{1}{2} - \sin^2\theta_W + \frac{5}{9}(1+r)\sin^4\theta_W, \tag{1}$$

$$R^{\overline{\nu}} \equiv \frac{\sigma(\overline{\nu}_\mu N \to \overline{\nu}_\mu X)}{\sigma(\overline{\nu}_\mu N \to \mu^+ X)} = \frac{1}{2} - \sin^2\theta_W + \frac{5}{9}(1+\frac{1}{r})\sin^4\theta_W, \tag{2}$$

where

$$r \equiv \frac{\sigma(\overline{\nu}_\mu N \to \mu^+ X)}{\sigma(\nu_\mu N \to \mu^- X)} \sim \frac{1}{2}, \tag{3}$$

The above equations are exact only for tree level scattering off an idealized isoscalar target composed of first generation light quarks. Corrections must be made for the non-isoscalar target, the heavy quark content of the nucleon, radiative effects, higher-twist processes, the longitudinal structure function (R_L), and charm production. This last effect is most important. Unfortunately, previous determinations of $\sin^2\theta_W$ measured in this way were subject to the same charm production uncertainties (resulting from imprecise knowledge of the charm quark mass) that dominated the CCFR error [1]. This ultimately limited the precision of neutrino measurements of electroweak parameters.

An alternate method for determining $\sin^2\theta_W$ that is much less dependent on the details of charm production and other sources of model uncertainty is derived from the Paschos-Wolfenstein quantity, R^- [3]:

$$R^- \equiv \frac{\sigma(\nu_\mu N \to \nu_\mu X) - \sigma(\overline{\nu}_\mu N \to \overline{\nu}_\mu X)}{\sigma(\nu_\mu N \to \mu^- X) - \sigma(\overline{\nu}_\mu N \to \mu^+ X)} = \frac{R^\nu - rR^{\overline{\nu}}}{1-r} = \frac{1}{2} - \sin^2\theta_W \tag{4}$$

Because R^- is formed from the difference of neutrino and antineutrino cross sections, almost all sensitivity to the effects of sea quark scattering cancels. This reduces the error associated with heavy quark production by roughly a factor of eight relative to the previous analysis. The substantially reduced uncertainties, however, come at a price. Unlike R^ν, the ratio R^- is more difficult to measure experimentally because neutral-current neutrino and antineutrino events have identical observed final states. The two samples can only be separated via *a priori* knowledge of the incoming neutrino beam type.

III. THE NEUTRINO BEAM AND THE NUTEV DETECTOR

High-purity neutrino and antineutrino beams were provided by the Sign Selected Quadrupole Train (SSQT) at the Fermilab Tevatron during the 1996-1997 fixed target run. Neutrinos are produced from the decay of pions and kaons resulting from interactions of 800 GeV protons in a BeO target. Dipole magnets immediately downstream of the proton target bend pions and kaons of specified charge in the direction of the NuTeV detector, while wrong-sign and neutral mesons are stopped in beam dumps. The resulting beam is almost purely neutrino or antineutrino depending on the selected sign of the parent mesons. The measured $\overline{\nu}_\mu$ contamination in the ν_μ beam is less than 1/1000 and the ν_μ contamination in the $\overline{\nu}_\mu$ beam is less than 1/500. In addition, the beam is almost purely muon-neutrino with a small contamination of electron neutrinos (1.3% in neutrino mode and 1.1% in antineutrino mode).

Neutrino interactions are then observed in the NuTeV detector, which is located approximately 1.5 km downstream of the proton target. The detector consists of an 18m long, 690 ton steel-scintillator target followed by an instrumented iron-toroid spectrometer (Figure 1). The target calorimeter is composed of 168 3 m x 3 m x 5.1 cm steel plates interspersed with liquid scintillation counters (spaced every two plates) and drift chambers (spaced every four plates). The scintillation counters provide triggering information as well as a determination of the longitudinal event vertex, event length and visible energy deposition. The mean position of hits in the drift chambers help establish the transverse event vertex. The toroidal spectrometer, which determines muon sign and momentum, is not directly used for this analysis.

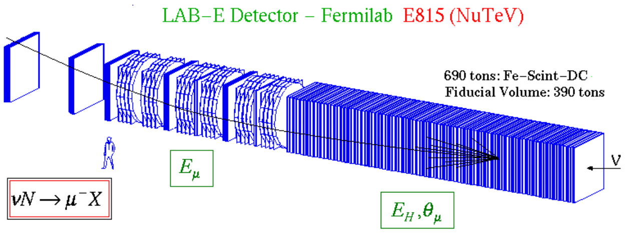

FIG. 1. The NuTev detector.

The detector was continuously calibrated through exposure to a wide energy range of test beam hadrons, electrons and muons delivered in a separate beamline during each accelerator cycle.

IV. EVENT SELECTION

For inclusion in this analysis, events must deposit at least 20 GeV of visible energy in the detector. This cut ensures full efficiency of the event trigger, proper vertex determination, and reduction of cosmic ray background events. Events must also have a vertex that lies within a 1.0 m box around the center of the detector which is at least 0.4 m of steel from the upstream end and 2.4 m of steel from the downstream end of the detector. This "box cut" ensures shower containment and minimizes the contribution from ν_e interactions. The chosen longitudinal fiducial volume ensures both that the event is neutrino-induced and that a meaningful event length can be measured. After all cuts, the total analysis sample consists of 1.3 million neutrino and 0.3 million antineutrino events with a mean energy of approximately 125 GeV.

V. EVENT SEPARATION

In order to measure $\sin^2\theta_W$, observed neutrino events must be separated into charged current (CC) and neutral current (NC) categories. Figure 2 shows typical CC and NC candidate events in the NuTeV detector.

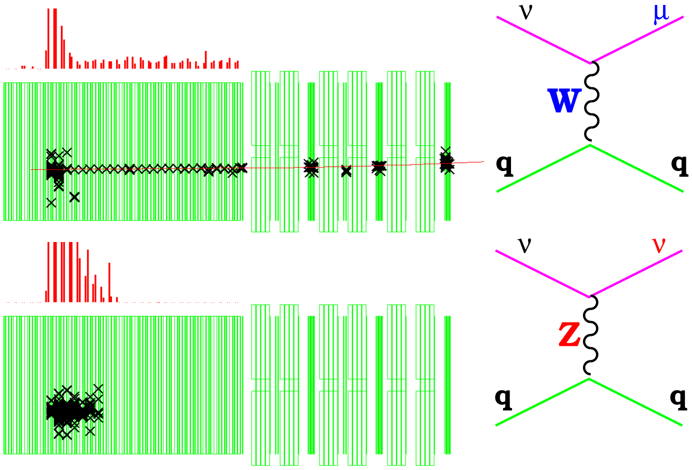

FIG. 2. Event displays of a NuTeV charged current candidate event (top) and neutral current candidate (bottom).

Both CC and NC neutrino interactions initiate a cascade of hadrons in the target that is registered in both the scintillation counters and drift chambers. Muon-neutrino CC events are distinguished by the presence of a final state muon. The muon typically penetrates well beyond the hadronic shower and deposits energy characteristic of a minimum-ionizing particle in a large number of scintillation counters. The muon track is clearly visible in the CC event at the top of Figure 2. On the other hand, there is no final state muon in muon-neutrino NC events; the final state neutrino is invisible, so ν_μ NC events can only be recognized by their hadronic shower.

Given the differing event topologies, one can statistically separate CC and NC interactions on the basis of event length (*i.e.*, on the presence or absence of a muon in an event). The length of an event is based on the longitudinal energy deposition in the calorimeter and is simply the number of scintillation counters spanned by the event. Events with a long length (spanning >20 counters) are identified as CC candidates and events with a short length (spanning ≤ 20 counters) are identified as NC candidates. The experimental quantity that is measured in both modes is the ratio:

$$R_{\mathrm{meas}} = \frac{\#\ \text{SHORT events}}{\#\ \text{LONG events}} = \frac{\#\ \text{NC candidates}}{\#\ \text{CC candidates}} \tag{5}$$

Neither sample is of course entirely pure. Long events are predominantly ν_μ CC interactions but contain small contaminations from both ν_μ NC events where the hadronic shower fluctuates to long lengths, as well as muons which are produced in upstream neutrino interactions in the shielding and later undergo a hard bremsstrahlung interaction in the detector. Short events are primarily ν_μ NC interactions but also contain contributions from low energy ν_μ CC events in which the muon ranges out, wide angle ν_μ CC events in which the muon exits the side of the detector, ν_e CC events and cosmic rays. The ratios (R_{meas}) of short to long events measured from the NuTeV data, are 0.4198 ± 0.0008 in the neutrino beam and 0.4215 ± 0.0017 in the antineutrino beam. A Standard Model value of $\sin^2\theta_W$ can be directly extracted from these measured ratios by using a detailed Monte Carlo simulation of the experiment. The Monte Carlo must include the integrated neutrino fluxes, the neutrino cross section as well as a detailed description of the NuTeV detector. The following sections will discuss these three components.

VI. THE MUON-NEUTRINO AND ELECTRON-NEUTRINO FLUXES

The Monte Carlo simulation requires neutrino flux information as input. In particular, a precise determination of the electron neutrino contamination in the beam is essential. The measured short to long ratios are directly impacted by the presence of electron neutrinos in the data sample because ν_e charged current interactions, which usually lack an energetic muon in the final state, are almost always identified as neutral current interactions in the detector.

The electron neutrino flux is estimated using a detailed beam Monte Carlo. Most of the observed ν_e's result from $K^\pm \to \pi^0 e^\pm \overset{(-)}{\nu}_e$ decay. The beam simulation can be tuned to describe ν_e and $\overline{\nu}_e$ production from charged kaon decay with high accuracy given that the $K^\pm$ decay contribution is well constrained from measurements of the observed ν_μ and $\overline{\nu}_\mu$ fluxes (as shown in Figure 3). Because of the precise alignment of the beamline elements and the low acceptance for neutral particle propagation in the SSQT, the largest uncertainty in the calculated electron neutrino flux results from the 1.5% uncertainty in the $K^\pm \to \pi^0 e^\pm \overset{(-)}{\nu}_e$ branching ratio. The result is a factor of three reduction in the electron-neutrino flux uncertainty when compared to CCFR.

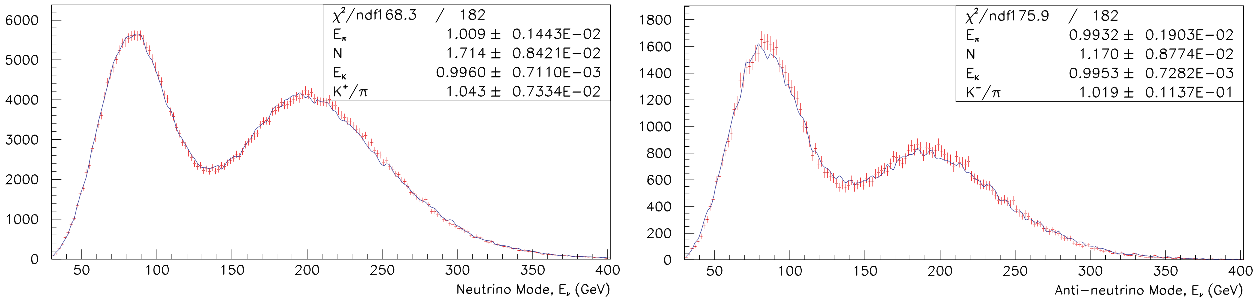

FIG. 3. ν_μ and $\overline{\nu}_\mu$ energy spectra comparing data (points) and the tuned beam Monte Carlo (histogram).

VII. CROSS SECTION MODEL

Neutrino-nucleon deep-inelastic scattering processes are simulated using a leading order cross section model. The cross section model incorporates leading order parton momentum distributions measured using the same target and cross section model as NuTeV [4]. Small modifications adjust the parton densities to produce the inherent up-down quark asymmetry consistent with muon scattering [5] and Drell-Yan [6] data. A leading order analysis of dimuon events in CCFR [7] provides the shape and magnitude of the strange sea. Mass suppression from charged-current charm production is modeled using a leading order slow-rescaling formalism whose parameters are measured from the same high-statistics dimuon sample. Electroweak and QED radiative corrections to the scattering cross sections are applied using radiative correction routines supplied by D. Yu. Bardin [8]. Higher twist contributions are quantified using a Vector-Dominance-Model as implemented by Pumplin [13] and constrained by lepto-production data [12]. A global analysis performed by L. Whitlow [14] provides a parameterization of the longitudinal structure function, R_L.

VIII. DETECTOR RESPONSE

The Monte Carlo must also accurately simulate the response of the detector to the product of neutrino interactions in the target. The critical detector parameters that must be modeled are the calorimeter response to muons, measurement of the neutrino interaction vertex, and the range of hadronic showers in the calorimeter. Precise determination of the various detector effects are made possible through extensive use of both neutrino data and large samples of calibration beam data. The efficiency, noise, and effective size of the scintillation counters are measured using neutrino data or test beam muons. Vertex finding resolutions and biases are studied using neutrino data combined with information from a detailed GEANT-based simulation of the detector. Test beam pion data provides information on hadronic shower lengths.

IX. EVENT LENGTH DISTRIBUTIONS

An important test of the Monte Carlo is its ability to predict the length distribution of events in the detector. Figure 4 shows event length distributions of the final data sample compared to the Monte Carlo prediction assuming the best-fit $\sin^2\theta_W$ (see next section). Events reaching the toroid, which comprise about 80% of the CC sample, have been left out for clarity but are included in the normalization of the Monte Carlo to the data. Data and MC agree well in each beam mode.

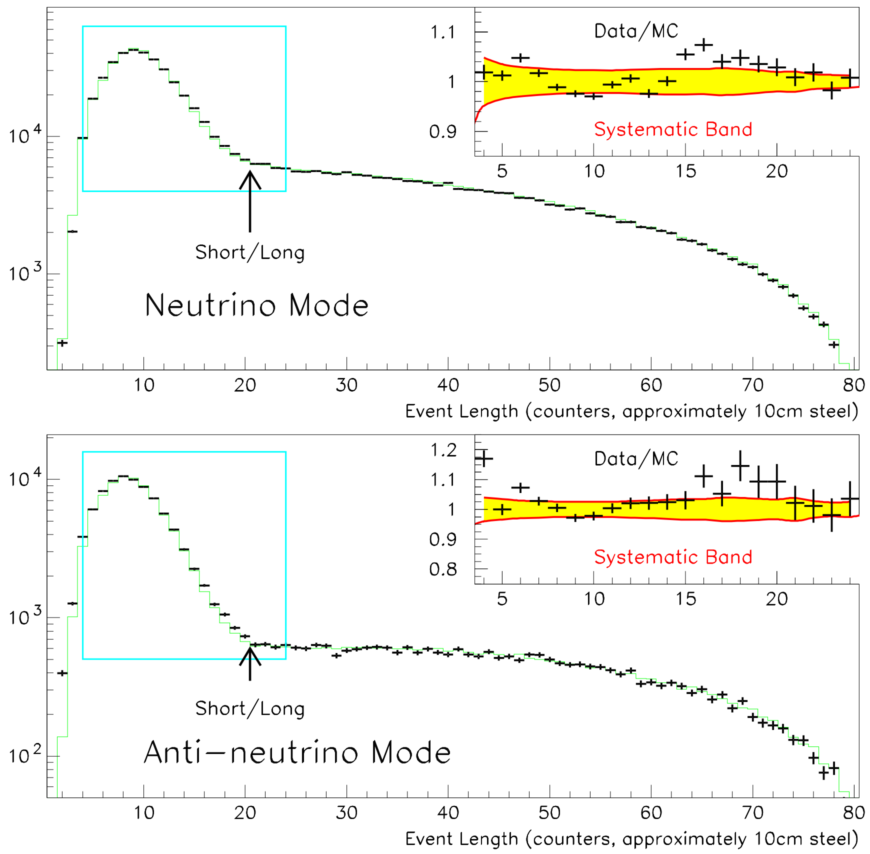

FIG. 4. Event length comparisons for neutrino and antineutrino events. The solid curve is the Monte Carlo prediction. The neutral current to charged current event separation (indicated by the arrow) is made at a length of 20 counters, approximately 2m of steel.

X. EXTRACTION OF $\sin^2\theta_W$

Given separate high-purity neutrino and antineutrino data sets, NuTeV measures the following linear combination of R^ν and $R^{\overline{\nu}}$:

$$R^- = R^\nu - xR^{\overline{\nu}}, \tag{6}$$

where x is chosen to be 0.5316. This value is obtained using Monte Carlo to minimize the dependence of R^- on the charm quark mass. This approach explicitly minimizes uncertainties related to the suppression of charm quark production, largely eliminates uncertainties related to sea quark scattering, and reduces many of the theoretical and detector uncertainties common to both the neutrino and antineutrino samples. The single remaining free parameter in the Monte Carlo, $\sin^2\theta_W$, is then varied until the model calculation of R^- agrees with what is measured in the data. The preliminary result from the NuTeV data sample for $M_{\rm top}$=175 GeV and $M_{\rm Higgs}$=150 GeV is:

$$\sin^2\theta_W^{(\rm on-shell)} = 0.2253 \pm 0.0019({\rm stat.}) \pm 0.0010({\rm syst.}) \tag{7}$$

Leading terms in the one-loop electroweak radiative corrections [8] to the W and Z self-energies produce a small residual dependence of our result on $M_{\rm top}$ and $M_{\rm Higgs}$. We explicitly quote the dependence of our measurement on the top and Higgs masses. The effect is small given the existing uncertainty on the top quark mass and the logarithmic dependence on the Higgs mass. For example, the total change in $\sin^2\theta_W$ from varying the Higgs mass from 100 GeV to 1 TeV is only 0.0005 (as is indicated by the shaded gray bands outlining the NuTeV result in Figure 6).

$$\delta\sin^2\theta_W = -0.00435\left[\left(\frac{M_{\rm top}}{175GeV}\right)^2 - 1\right] + 0.00048\log\frac{M_{\rm Higgs}}{150GeV}. \tag{8}$$

Having chosen the convention, $\sin^2\theta_W^{(\rm on-shell)} \equiv 1 - \frac{M_W^2}{M_Z^2}$, where M_W and M_Z are the physical gauge boson masses, our result implies:

$$M_W = 80.26 \pm 0.10({\rm stat.}) \pm 0.05({\rm syst.}) = 80.26 \pm 0.11{\rm GeV} \tag{9}$$

A comparison of this result with direct measurements of M_W is shown in Figure 5. Our measurement is in good agreement with Standard Model expectations and is consistent with the most recent measurements from W and Z production as well as from other neutrino experiments (Figure 6).

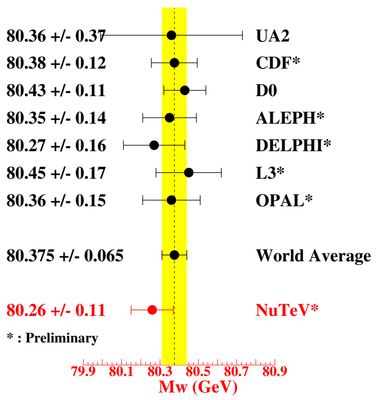

FIG. 5. Direct W boson mass measurements compared with this result (at the time of DPF99).

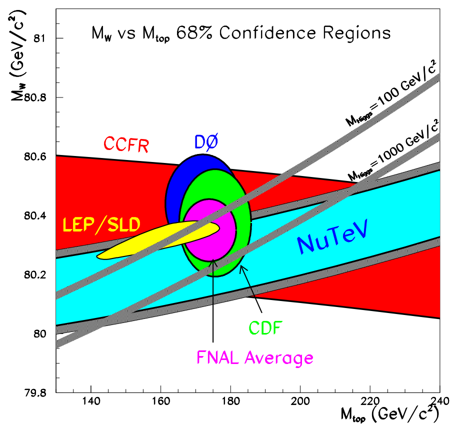

FIG. 6. Experimental constraints presented on the M_W-$M_{\rm top}$ plane (at the time of DPF99). The two narrow lines indicate the Standard Model predictions for $M_{\rm Higgs}$=100 and 1000 GeV.

If these plots are now updated to include new measurements from CDF [9], DØ [10] and LEP [11] that were presented at Electroweak Moriond in March of this year, it is interesting to note that tighter constraints on the Higgs mass are beginning to emerge (Figure 8).

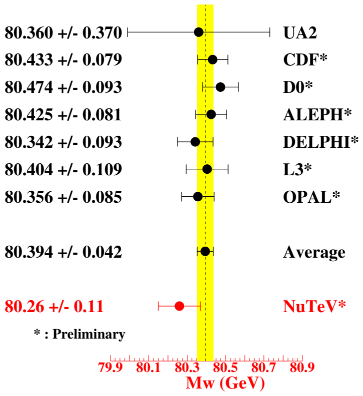

FIG. 7. Direct W boson mass measurements compared with this result (updated to include new measurements presented at EW Moriond99).

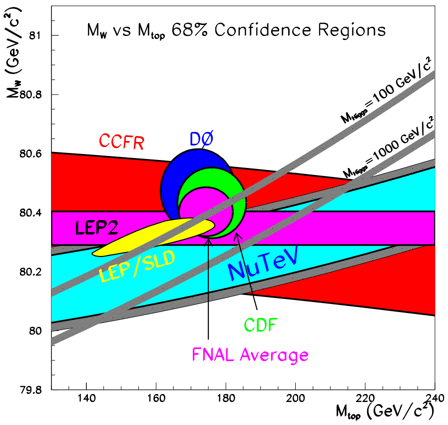

FIG. 8. Experimental constraints presented on the M_W-$M_{\rm top}$ plane (updated to include new measurements presented at EW Moriond99).

XI. CONCLUSIONS

NuTeV has successfully completed its data-taking and has extracted a preliminary value of $\sin^2\theta_W$. The precision of this result is a factor of two improvement over previous measurements in νN scattering because of reduced systematics associated with measuring the Paschos Wolfenstein ratio, R^-. Interpreted within the framework of the Standard Model, this result is equivalent to a determination of the W mass and is consistent with direct measurements of M_W.

[1] K.S. McFarland, *et al.*, Eur. Phys. Jour. **C31**, 509 (1998).
[2] C.H. Llewellyn Smith, Nucl. Phys. **B228**, 205 (1983).
[3] E.A. Paschos and L. Wolfenstein, Phys. Rev. **D7**, 91 (1973).
[4] W.G. Seligman, *et al.*, Phys. Rev. Lett. **79**, 1213 (1997).
[5] M. Arneodo, *et al.*, Nucl. Phys., **B487**, 3 (1997)
[6] E.A. Hawker, *et al.*, Phys. Rev. Lett. **80**, 3715 (1998).
[7] S.A. Rabinowitz, *et al.*, Phys. Rev. Lett **70**, 134 (1993).
[8] D. Yu. Bardin, V.A. Dokuchaeva, JINR-E2-86-260 (1986).
[9] Y. Kim for the CDF collaboration, proceedings of La Thuile 1999.
[10] A. Kotwal for the DØcollaboration, DØNote 3544 (1999).
[11] LEP Electroweak Working Group, LEPEWWG/WW/99-01, revised (1999).
[12] M. Virchaux and A. Milsztajn, Phys. Lett. **B274**, 221 (1992).
[13] J. Pumplin, Phys. Rev. Lett. **64**, 2751 (1990).
[14] L.W. Whitlow, SLAC-REPORT-357, 109 (1990).